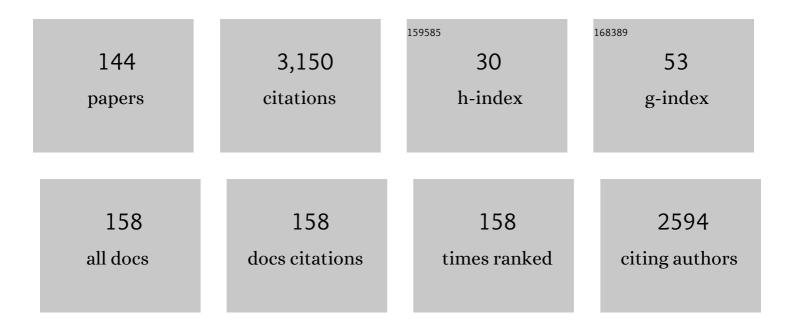
## Juha Lemmetyinen

List of Publications by Year in descending order

Source: https://exaly.com/author-pdf/9305021/publications.pdf Version: 2024-02-01



#	Article	IF	CITATIONS
1	Estimating northern hemisphere snow water equivalent for climate research through assimilation of space-borne radiometer data and ground-based measurements. Remote Sensing of Environment, 2011, 115, 3517-3529.	11.0	481
2	Patterns and trends of Northern Hemisphere snow mass from 1980 to 2018. Nature, 2020, 581, 294-298.	27.8	203
3	Detection of soil freezing from L-band passive microwave observations. Remote Sensing of Environment, 2014, 147, 206-218.	11.0	120
4	SMOS prototype algorithm for detecting autumn soil freezing. Remote Sensing of Environment, 2016, 180, 346-360.	11.0	109
5	L-Band Radiometer Observations of Soil Processes in Boreal and Subarctic Environments. IEEE Transactions on Geoscience and Remote Sensing, 2012, 50, 1483-1497.	6.3	106
6	Multiple-Layer Adaptation of HUT Snow Emission Model: Comparison With Experimental Data. IEEE Transactions on Geoscience and Remote Sensing, 2010, 48, 2781-2794.	6.3	97
7	Snow Water Equivalent of Dry Snow Measured by Differential Interferometry. IEEE Journal of Selected Topics in Applied Earth Observations and Remote Sensing, 2015, 8, 3773-3790.	4.9	86
8	Evaluation of snow products over the Tibetan Plateau. Hydrological Processes, 2015, 29, 3247-3260.	2.6	84
9	Early snowmelt significantly enhances boreal springtime carbon uptake. Proceedings of the National Academy of Sciences of the United States of America, 2017, 114, 11081-11086.	7.1	84
10	Observed and modelled effects of ice lens formation on passive microwave brightness temperatures over snow covered tundra. Remote Sensing of Environment, 2010, 114, 116-126.	11.0	74
11	Evaluation of passive microwave brightness temperature simulations and snow water equivalent retrievals through a winter season. Remote Sensing of Environment, 2012, 117, 236-248.	11.0	65
12	Model for microwave emission of a snow-covered ground with focus on L band. Remote Sensing of Environment, 2014, 154, 180-191.	11.0	62
13	Snow density and ground permittivity retrieved from L-band radiometry: Application to experimental data. Remote Sensing of Environment, 2016, 180, 377-391.	11.0	60
14	Snow Density and Ground Permittivity Retrieved from L-Band Radiometry: A Synthetic Analysis. IEEE Journal of Selected Topics in Applied Earth Observations and Remote Sensing, 2015, 8, 3833-3845.	4.9	59
15	GlobSnow v3.0 Northern Hemisphere snow water equivalent dataset. Scientific Data, 2021, 8, 163.	5.3	58
16	Modeling Both Active and Passive Microwave Remote Sensing of Snow Using Dense Media Radiative Transfer (DMRT) Theory With Multiple Scattering and Backscattering Enhancement. IEEE Journal of Selected Topics in Applied Earth Observations and Remote Sensing, 2015, 8, 4418-4430.	4.9	53
17	MEMLS3&a: Microwave Emission Model of Layered Snowpacks adapted to include backscattering. Geoscientific Model Development, 2015, 8, 2611-2626.	3.6	52
18	Response of L-Band brightness temperatures to freeze/thaw and snow dynamics in a prairie environment from ground-based radiometer measurements. Remote Sensing of Environment, 2017, 191, 67-80.	11.0	50

#	Article	IF	CITATIONS
19	Dense Media Radiative Transfer Applied to SnowScat and SnowSAR. IEEE Journal of Selected Topics in Applied Earth Observations and Remote Sensing, 2014, 7, 3811-3825.	4.9	44
20	Anisotropy of seasonal snow measured by polarimetric phase differences in radar time series. Cryosphere, 2016, 10, 1771-1797.	3.9	43
21	Retrieval of Effective Correlation Length and Snow Water Equivalent from Radar and Passive Microwave Measurements. Remote Sensing, 2018, 10, 170.	4.0	42
22	Physical properties of Arctic versus subarctic snow: Implications for high latitude passive microwave snow water equivalent retrievals. Journal of Geophysical Research D: Atmospheres, 2014, 119, 7254-7270.	3.3	39
23	A Comparison of Airborne Microwave Brightness Temperatures and Snowpack Properties Across the Boreal Forests of Finland and Western Canada. IEEE Transactions on Geoscience and Remote Sensing, 2009, 47, 965-978.	6.3	38
24	Simulating seasonally and spatially varying snow cover brightness temperature using HUT snow emission model and retrieval of a microwave effective grain size. Remote Sensing of Environment, 2015, 156, 71-95.	11.0	37
25	Nordic Snow Radar Experiment. Geoscientific Instrumentation, Methods and Data Systems, 2016, 5, 403-415.	1.6	37
26	Estimating Snow Water Equivalent with Backscattering at X and Ku Band Based on Absorption Loss. Remote Sensing, 2016, 8, 505.	4.0	37
27	The influence of snow microstructure on dual-frequency radar measurements in a tundra environment. Remote Sensing of Environment, 2018, 215, 242-254.	11.0	37
28	Comparison of traditional and optical grain-size field measurements with SNOWPACK simulations in a taiga snowpack. Journal of Glaciology, 2015, 61, 151-162.	2.2	33
29	A 7-year dataset for driving and evaluating snow models at an Arctic site (SodankyläFinland). Geoscientific Instrumentation, Methods and Data Systems, 2016, 5, 219-227.	1.6	32
30	SMOS Calibration Subsystem. IEEE Transactions on Geoscience and Remote Sensing, 2007, 45, 3691-3700.	6.3	31
31	Estimation of ice thickness on large northern lakes from AMSR-E brightness temperature measurements. Remote Sensing of Environment, 2014, 150, 1-19.	11.0	31
32	The Effect of Boreal Forest Canopy in Satellite Snow Mapping—A Multisensor Analysis. IEEE Transactions on Geoscience and Remote Sensing, 2015, 53, 6593-6607.	6.3	30
33	Forward and Inverse Radar Modeling of Terrestrial Snow Using SnowSAR Data. IEEE Transactions on Geoscience and Remote Sensing, 2018, 56, 7122-7132.	6.3	30
34	Snow depth estimation and historical data reconstruction over China based on a random forest machine learning approach. Cryosphere, 2020, 14, 1763-1778.	3.9	30
35	The Sodankylän situ soil moisture observation network: an example application of ESAÂCCI soil moisture product evaluation. Geoscientific Instrumentation, Methods and Data Systems, 2016, 5, 95-108.	1.6	28
36	Implications of boreal forest stand characteristics for X-band SAR flood mapping accuracy. Remote Sensing of Environment, 2016, 186, 47-63.	11.0	28

#	Article	IF	CITATIONS
37	Differences Between the HUT Snow Emission Model and MEMLS and Their Effects on Brightness Temperature Simulation. IEEE Transactions on Geoscience and Remote Sensing, 2016, 54, 2001-2019.	6.3	28
38	Microstructure representation of snow in coupled snowpack and microwave emission models. Cryosphere, 2017, 11, 229-246.	3.9	28
39	MODIS-based Daily Lake Ice Extent and Coverage dataset for Tibetan Plateau. Big Earth Data, 2019, 3, 170-185.	4.4	27
40	Snow stratigraphic heterogeneity within groundâ€based passive microwave radiometer footprints: Implications for emission modeling. Journal of Geophysical Research F: Earth Surface, 2014, 119, 550-565.	2.8	24
41	Observations and Simulation of Multifrequency SAR Data Over a Snow-Covered Boreal Forest. IEEE Journal of Selected Topics in Applied Earth Observations and Remote Sensing, 2016, 9, 1216-1228.	4.9	23
42	Impact of dynamic snow density on GlobSnow snow water equivalent retrieval accuracy. Cryosphere, 2021, 15, 2969-2981.	3.9	22
43	Validation of remotely sensed estimates of snow water equivalent using multiple reference datasets from the middle and high latitudes of China. Journal of Hydrology, 2020, 590, 125499.	5.4	21
44	Correcting for the influence of frozen lakes in satellite microwave radiometer observations through application of a microwave emission model. Remote Sensing of Environment, 2011, 115, 3695-3706.	11.0	20
45	Evaluation of the HUT modified snow emission model over lake ice using airborne passive microwave measurements. Remote Sensing of Environment, 2011, 115, 233-244.	11.0	19
46	The Influence of Thermal Properties and Canopy- Intercepted Snow on Passive Microwave Transmissivity of a Scots Pine. IEEE Transactions on Geoscience and Remote Sensing, 2019, 57, 5424-5433.	6.3	18
47	New Snow Water Equivalent Processing System With Improved Resolution Over Europe and its Applications in Hydrology. IEEE Journal of Selected Topics in Applied Earth Observations and Remote Sensing, 2017, 10, 428-436.	4.9	17
48	Experimental Study on Radiometric Performance of Synthetic Aperture Radiometer HUT-2D—Measurements of Natural Targets. IEEE Transactions on Geoscience and Remote Sensing, 2011, 49, 814-826.	6.3	16
49	Snow Density and Ground Permittivity Retrieved From L-Band Radiometry: A Retrieval Sensitivity Analysis. IEEE Journal of Selected Topics in Applied Earth Observations and Remote Sensing, 2017, 10, 3148-3161.	4.9	16
50	Spatially Distributed Evaluation of ESA CCI Soil Moisture Products in a Northern Boreal Forest Environment. Geosciences (Switzerland), 2018, 8, 51.	2.2	16
51	Coupling SNOWPACK-modeled grain size parameters with the HUT snow emission model. Remote Sensing of Environment, 2017, 194, 33-47.	11.0	15
52	Observation and Modeling of the Microwave Brightness Temperature of Snow-Covered Frozen Lakes and Wetlands. IEEE Transactions on Geoscience and Remote Sensing, 2014, 52, 3275-3288.	6.3	14
53	A Modeling-Based Approach for Soil Frost Detection in the Northern Boreal Forest Region With C-Band SAR. IEEE Transactions on Geoscience and Remote Sensing, 2019, 57, 1069-1083.	6.3	14
54	Spatial Variability of L-Band Brightness Temperature during Freeze/Thaw Events over a Prairie Environment. Remote Sensing, 2017, 9, 894.	4.0	13

#	Article	IF	CITATIONS
55	Exploiting the ANN Potential in Estimating Snow Depth and Snow Water Equivalent From the Airborne SnowSAR Data at X- and Ku-Bands. IEEE Transactions on Geoscience and Remote Sensing, 2022, 60, 1-16.	6.3	13
56	Temperature effects on L-band vegetation optical depth of a boreal forest. Remote Sensing of Environment, 2021, 263, 112542.	11.0	12
57	Estimation of Microwave Atmospheric Transmittance Over China. IEEE Geoscience and Remote Sensing Letters, 2017, 14, 2210-2214.	3.1	11
58	Sentinel-1 based soil freeze/thaw estimation in boreal forest environments. Remote Sensing of Environment, 2021, 254, 112267.	11.0	10
59	Spatial and temporal variation of bulk snow properties in northern boreal and tundra environments based on extensive field measurements. Geoscientific Instrumentation, Methods and Data Systems, 2016, 5, 347-363.	1.6	9
60	Active Microwave Scattering Signature of Snowpack—Continuous Multiyear SnowScat Observation Experiments. IEEE Journal of Selected Topics in Applied Earth Observations and Remote Sensing, 2016, 9, 3849-3869.	4.9	8
61	Modelling the L-Band Snow-Covered Surface Emission in a Winter Canadian Prairie Environment. Remote Sensing, 2018, 10, 1451.	4.0	8
62	A lake ice phenology dataset for the Northern Hemisphere based on passive microwave remote sensing. Big Earth Data, 2022, 6, 401-419.	4.4	8
63	The atmosphere influence to AMSR-E measurements over snow-covered areas: Simulation and experiments. , 2009, , .		7
64	Investigating hemispherical trends in snow accumulation using GlobSnow snow water equivalent data. , 2011, , .		7
65	Solving Challenges of Assimilating Microwave Remote Sensing Signatures With a Physical Model to Estimate Snow Water Equivalent. Water Resources Research, 2021, 57, e2021WR030119.	4.2	7
66	Determination of Snow Emission on Lake Ice from Airborne Passive Microwave Measurements. , 2008, , .		6
67	Multifrequency microwave radiometry of snow on lake ice: Observations and simulations. , 2015, , .		6
68	Wet Snow Depth from Tandem-X Single-Pass Insar Dem Differencing. , 2018, , .		6
69	SodSAR: A Tower-Based 1–10 GHz SAR System for Snow, Soil and Vegetation Studies. Sensors, 2020, 20, 6702.	3.8	6
70	X-Ray Tomography-Based Microstructure Representation in the Snow Microwave Radiative Transfer Model. IEEE Transactions on Geoscience and Remote Sensing, 2022, 60, 1-15.	6.3	6
71	Inter-annual variation in lake ice composition in the European Arctic: observations based on high-resolution thermistor strings. Earth System Science Data, 2021, 13, 3967-3978.	9.9	6
72	Atmospheric Correction to Passive Microwave Brightness Temperature in Snow Cover Mapping Over China. IEEE Transactions on Geoscience and Remote Sensing, 2021, 59, 6482-6495.	6.3	6

#	Article	IF	CITATIONS
73	Analysis of active and passive microwave observations from the NoSREx campaign. , 2011, , .		5
74	Calibration subsystem for spaceborne interferometric radiometer. , 0, , .		4
75	Ground calibration of SMOS: NIR and CAS. , 2007, , .		4
76	The AMSR-E Instantaneous Emissivity Estimation and its Correlation, Frequency Dependency Analysis over Different Land Covers. , 2008, , .		4
77	Correction to "Multiple-Layer Adaptation of HUT Snow Emission Model: Comparison With Experimental Data―[Jul 10 2781-2794. IEEE Transactions on Geoscience and Remote Sensing, 2010, 48, 3055-3055.	6.3	4
78	Detection of a Sea Surface Salinity Gradient Using Data Sets of Airborne Synthetic Aperture Radiometer HUT-2-D and a GNSS-R Instrument. IEEE Transactions on Geoscience and Remote Sensing, 2011, 49, 4561-4571.	6.3	4
79	Multifrequency microwave radiometer measurements of snow on lake ice. , 2012, , .		4
80	Arctic Snow Microstructure Experiment for the development of snow emission modelling. Geoscientific Instrumentation, Methods and Data Systems, 2016, 5, 85-94.	1.6	4
81	Retrieval of snow parameters from L-band observations - application for SMOS and SMAP. , 2016, , .		4
82	Review Article: Global Monitoring of Snow Water Equivalent using High Frequency Radar Remote Sensing. , 0, , .		4
83	SMOS Calibration Subsystem. , 2006, , .		3
84	Error Propagation in Calibration Networks of Synthetic Aperture Radiometers. IEEE Transactions on Geoscience and Remote Sensing, 2009, 47, 3140-3150.	6.3	3
85	Analysis between AMSR-E swath brightness temperature and ground snow depth data in winter time over Tibet Plateau, China. , 2010, , .		3
86	Observing seasonal snow changes in the boreal forest area using active and passive microwave measurements. , 2010, , .		3
87	L-band measurements of boreal soil. , 2010, , .		3
88	Microwave emission signature of snow-covered lake ice. , 2011, , .		3
89	Analysis of the passive microwave high-frequency signal in the shallow snow retrieval. , 2011, , .		3
90	Refinement of the X and Ku band dual-polarization scatterometer snow water equivalent retrieval algorithm. , 2014, , .		3

#	Article	IF	CITATIONS
91	Derivation and Evaluation of a New Extinction Coefficient for Use With the n-HUT Snow Emission Model. IEEE Transactions on Geoscience and Remote Sensing, 2019, 57, 7406-7417.	6.3	3
92	Simulating the Influence of Temperature on Microwave Transmissivity of Trees During Winter Observed by Spaceborne Microwave Radiometery. IEEE Journal of Selected Topics in Applied Earth Observations and Remote Sensing, 2020, 13, 4816-4824.	4.9	3
93	The influence of tree transmissivity variations in winter on satellite snow parameter observations. International Journal of Digital Earth, 2021, 14, 1337-1353.	3.9	3
94	Effects of Arctic Wetland Dynamics on Tower-Based GNSS Reflectometry Observations. IEEE Transactions on Geoscience and Remote Sensing, 2022, 60, 1-17.	6.3	3
95	Attenuation of Radar Signal by a Boreal Forest Canopy in Winter. IEEE Geoscience and Remote Sensing Letters, 2022, 19, 1-5.	3.1	3
96	Airborne ocean wind vector measurement using 36.5 GHz profiling polarimetric radiometer. , 0, , .		2
97	Implementing hemispherical snow water equivalent product assimilating weather station observations and spaceborne microwave data. , 2011, , .		2
98	Bicontinuous/DMRT model applied to active and passive microwave remote sensing of terrestrial snow. , 2014, , .		2
99	Assessing global satellite-based snow water equivalent datasets in ESA SnowPEx project. , 2016, , .		2
100	Season -Length Observations of Active and Passive Microwave Signatures of Snow Cover in a Boreal Forest Environment. , 2018, , .		2
101	Smos Retrievals of Soil Freezing and Thawing and its Applications. , 2018, , .		2
102	Operational snow map production for whole eurasia using microwave radiometer and ground-based observations. , 2007, , .		1
103	Thermal stabilized front-end PCB with active cold calibration load for L-band radiometer. , 2007, , .		1
104	Sensitivity of Airborne 36.5-GHz Polarimetric Radiometer's Wind-Speed Measurement to Incidence Angle. IEEE Transactions on Geoscience and Remote Sensing, 2007, 45, 2122-2129.	6.3	1
105	Sea surface salinity retrieval demonstration using datasets of synthetic aperture radiometer HUT-2D. , 2009, , .		1
106	SNOWCARBO: Monitoring and assessment of carbon balance related phenomena in Finland and northern Eurasia. , 2011, , .		1
107	Monitoring snow parameters in boreal forest using multi-frequency SAR data. , 2014, , .		1
108	Comparison of SSMIS, AMSR-E and MWRI brightness temperature data. , 2014, , .		1

#	Article	IF	CITATIONS
109	Estimation of vegetation and soil backscattering for the retrieval of SWE in sparse forests. , 2015, , .		1
110	Snow on lake ice: Overview of a multiyear airborne radiometer data collection program and related modeling efforts. , 2016, , .		1
111	Microwave brightness temperature of snow: Observations and simulations. , 2016, , .		1
112	Assessment of Seasonal snow Cover Mass in Northern Hemisphere During the Satellite-ERA. , 2018, , .		1
113	Atmospheric correction of passive microwave brightness temperature on the estimation of snow depth. , 2019, , .		1
114	Comparative Analysis to the Lake Ice Phenology Changes of Mongolian Plateau, Tibetan Plateau and Northern Europe through Passive Microwave. , 2019, , .		1
115	Comparison to Changes of Lake Ice Phenology and Air Temperature over Northern Europe, Tibetan Plateau and Mongolian Plateau. IOP Conference Series: Earth and Environmental Science, 2020, 502, 012033.	0.3	1
116	Assessing the Performances of FY-3D/MWRI and DMSP SSMIS in GlobSnow-2 Assimilation System for SWE Estimation. , 2020, , .		1
117	Spatial Microwave Brightness Temperature Variations of Boreal Forests under Dry Snow Cover Conditions. , 0, , .		0
118	Experimental and modeling studies of microwave remote sensing of seasonal snow. , 2009, , .		0
119	Soil moisture retrieval from HUT-2D synthetic aperture radiometer data. , 2009, , .		0
120	Experimental validation activities of HUT snow emission model. , 2009, , .		0
121	Combined hemispherical scale SWE and snow clearance monitoring. , 2010, , .		Ο
122	Improving hydrological forecasting using multi-source remote sensing data together with in situ measurements. , 2010, , .		0
123	Experimental study on radiometric performance of synthetic aperture radiometer hut-2D – Measurements of natural targets. , 2010, , .		Ο
124	Effects of snowpack parameters and layering processes at X- and Ku-band backscatter. , 2011, , .		0
125	Synthetic aperture radiometer measurements of freezing soil. , 2011, , .		Ο
126	An emissivity-based land surface temperature retrieval algorithm. , 2012, , .		0

#	Article	IF	CITATIONS
127	Electromagnetic simulation and validation of backscattering from boreal forest in the C-Ku frequency range. , 2013, , .		Ο
128	Comparasion on snow depth algorithms over China using AMSR-E passive microwave remote sensing. , 2014, , .		0
129	Potential of L-band passive microwave radiometry for snow parameter retrieval. , 2015, , .		0
130	On the estimate of the microwave shadowing effect on sparse boreal forests. , 2015, , .		0
131	Analysis of L-Band brightness temperatures response to freeze/thaw in two prairie environments from surface-based radiometer measurements. , 2016, , .		Ο
132	Hydrological applications of super resolution SWE processing system over Europe. , 2016, , .		0
133	Centi- and millimeter-wave atmospheric transmittance estimation and analysis over China. , 2016, , .		Ο
134	Diurnal variation of brightness temperature of terrestrial snow during snowmelt. , 2016, , .		0
135	Consideration of variable atmospheric transmissivity in passive microwave snowpack retrievals over Tibetan Plateau. , 2016, , .		Ο
136	Long term changes in Northern hemisphere snow cover from SWE timeseries constrained with SE data. , 2017, , .		0
137	Future mission concepts for measuring snow mass. , 2017, , .		Ο
138	Validation of physical model and radar retrieval algorithm of snow water equivalent using SnowSAR data. , 2017, , .		0
139	Soil Permittivity and Soil Frost Retrievals Using a Synergistic Method for Active and Passive Microwave Instruments. , 2018, , .		0
140	Foreword to the Special Issue on MicroRad 2018. IEEE Journal of Selected Topics in Applied Earth Observations and Remote Sensing, 2019, 12, 1631-1632.	4.9	0
141	Development of SWE Retrieval Methods in the ESA Snow CCI Project And Long Term Trends in Seasonal Snow Mass. , 2019, , .		0
142	Estimation of Hemispheric Snow Mass Evolution Based on Microwave Radiometry. , 2021, , .		0
143	Development of Dynamic Snow Density Methodology for GlobSnow SWE Retrieval. , 2021, , .		0
144	Modeling Climate Sensitive Infectious Diseases in the Arctic Springer Polar Sciences 2021 93-111	0.1	0

144 Modeling Climate Sensitive Infectious Diseases in the Arctic. Springer Polar Sciences, 2021, , 93-111. 0.1